CHITOSAN-BASED BIOCOMPOSITE HYDROGELS WITH SQUID PEN PROTEIN FOR ANIONIC DYES ADSORPTION

Pedro Y. S. Nakasu[‡1], Maite A. Martinez[‡1],Talia Shmool[1], Susiana Melanie[1], Jason P. Hallett[1]

[1]Department of Chemical Engineering, Imperial College London, SW7 2AZ, London

‡These authors contributed equally

KEYWORDS: reactive blue 4, methyl orange, squid waste, wastewater treatment, biomaterials.

ABSTRACT: Growing environmental concerns have spurred the search for sustainable solutions to water pollution, particularly focusing on the removal of persistent synthetic dyes from wastewater. Hydrogels, known for their water-absorbing capabilities, have emerged as promising materials for such applications. This study investigates the use of squid pen protein (SPP) and chitosan, two biodegradable and biocompatible polymers, in fabricating hydrogels for effective anionic dye removal. SPP, derived from squid pen is a marine waste product and a sustainable alternative to traditional synthetic polymers. When combined with chitosan, extracted from crustacean exoskeletons, the resulting hydrogels demonstrate enhanced dye sorption properties due to the complementary characteristics of the two materials. The study focuses on synthesizing and characterizing SPP-chitosan hydrogels, assessing their effectiveness in removing reactive blue 4 (RB4) and methyl orange (MO) dyes from aqueous solutions. The hydrogels achieved a maximum swelling ratio of 140.7%, with adsorption capacities of 153.85 mg/g for RB4 and 60.24 mg/g for MO. These results were characterized using Fourier-transform infrared spectroscopy, optical microscopy, and scanning electron microscopy, providing insights into the functional groups and surface structures involved in the dye removal process. The study also highlights that a higher crosslinker content negatively impacts adsorption performance by reducing the availability of binding sites on the protein and chitosan. The combination of SPP with chitosan potentially presents a cost-effective and environmentally sustainable alternative for wastewater treatment, offering a promising solution for mitigating water pollution through sustainable materials.

In the wake of escalating environmental concerns, the quest for sustainable and eco-friendly solutions to water pollution has intensified (1). Among the myriad pollutants, synthetic dyes pose a significant challenge due to their persistence and adverse effects on ecosystems and human health (2). Addressing this challenge necessitates innovative approaches that not only efficiently remove dyes from wastewater but also adhere to principles of environmental sustainability.

Hydrogels, three-dimensional networks capable of absorbing and retaining large volumes of water or aqueous solutions, have emerged as promising materials for wastewater treatment (2,3). Given the tunable properties of hydrogels, these are attractive candidates for environmental remediation applications. Particularly, the synthesis of biocomposites offers a compelling avenue for designing hydrogels with enhanced functionality for dye removal due to the biocompatibility and biodegradability of hydrogels (4).

In this study, we explore the synergistic potential of squid pen protein (SPP) and chitosan, two biocompatible and biodegradable polymers, in the fabrication of hydrogels tailored for the removal of anionic dyes from aqueous solutions. Squid pen protein (SPP), a promising stream extracted from squid pen, is readily available and an inexpensive marine waste composed of mainly 75wt% protein and 25wt% chitin (5). It offers a sustainable alternative to traditional synthetic polymers. When combined with chitosan, derived from the exoskeletons of crustaceans, the resulting hydrogels exhibit promising characteristics for dye sorption, owing to the complementary properties of the constituent polymers (2).

The rationale behind this approach stems from the imperative to harness natural resources efficiently while mitigating the environmental footprint of wastewater treatment processes. Squid pen can be used to produce chitosan and the protein is extracted from the pen with alkaline solutions that become wastewater, which negatively impact the process and the environment (6). By leveraging the unique amino acid functionalities of SPP and the structural integrity of chitosan-based materials, we aim to develop hydrogels that not only demonstrate superior dye removal efficiency but also align with the principles of green chemistry and circular economy. Additionally, chitosan cost can be as high as 200 USD per kg (25), and with up to 50wt% of chitosan being substituted by an inexpensive squid waste and outperforming the pure chitosan hydrogels, we can upscale squid waste utilisation in a more economically feasible manner.

This paper delineates the synthesis and characterization of SPP-chitosan hydrogels and investigates their efficacy in removing the anionic dyes reactive blue 4 (RB4) and methyl orange (MO) (structures shown in Fig S1 and S2 in ESI) from aqueous solutions. Through a systematic analysis of the physicochemical properties and dye sorption kinetics of the hydrogels, we elucidate the underlying mechanisms governing the dye removal process. Furthermore, we discuss the implications of our findings in the context of sustainable wastewater treatment strategies and outline potential avenues for future research.

RESULTS AND DISCUSSION

We produced the biocomposite hydrogels by homogenizing both the SPP and chitosan in diluted acetic acid, then, a certain amount of the crosslinker, glutaraldehyde, was added. The final solution was then freeze-dried to yield a spongy-foamy hydrogel that later was hydrated for the dye adsorption experiments. The complete synthesis procedure of the hydrogels are described in the ESI.

We employed design of experiments (DOE) to identify the optimal combination of component concentrations to produce hydrogels with superior dye adsorption capacity and physical attributes. For the synthesis of the SPP hydrogels, 11 different experiments were conducted consisting of 8 runs and 3 centre point replicates. The chitosan to protein percentage ratio, X1, ranged from 50 to 70 wt%; the crosslinking percentage content, X2, from 1 to 3 wt%; and the total solids loading, X3, from 1 to 5 wt%. The complete experimental matrix is shown in table S1 (ESI). The samples were named after the DoE factors: X1_X2_X3, for instance, a sample with chitosan to protein ratio, X1, of 70%, crosslinker percentage, X2, of 2% and total solid loading, X3, of 5% will be named sample 70_2_5. To validate the contributions of the added proteins to enhance adsorption capacity and physical strength, hydrogels with only chitosan were also prepared. Their formulation included a solid loading of 3% chitosan and 2% crosslinker, reflecting the center points from the DOE.

Once manufactured, the hydrogels underwent various tests to evaluate the effects of the selected variables and their combinations on the characteristics and capacities of the hydrogels. These tests included mechanical strength, physical stability, water swelling ratio, and dye adsorption capacity. The complete characterization procedure of the gels is described in the ESI.

3.1. Water absorption capacity

The chitosan hydrogels (CH-1, CH-2, and CH-3) exhibited an average swelling of 110.7%. In contrast, the squid pen protein hydrogels (60_2_3, 70_3_50, and 70_3_51) demonstrated average swelling of 139.7 wt%. This increase in absorption capacity is attributed to the addition of each protein, which enhances the desirability as adsorbents of the hydrogels.

Moreover, it was observed that the solid loading significantly affects the swelling for both squid pen and BSG protein hydrogels. The squid pen protein hydrogels with a 5% solid loading (70_3_5, 70_1_5, 50_3_5, and 50_1_5) and a 1% solid loading (70_3_1, 70_1_1, 50_3_1, and 50_1_1) exhibited average swelling of 140.7% and 71.7%, respectively. Overall, the protein-containing hydrogels with the lowest solid loading exhibited inferior results compared to even the chitosan hydrogels, indicating that this composition does not yield valuable and efficient hydrogels in terms of absorption capacity.

Furthermore, standard chitosan and acetic acid hydrogels have a water absorption capacity range of 90-600%, depending on the additional materials included in the formulation (7). In a study by (8) with chitosan-graft-poly(acrylic acid), synthesize gels had up to 160 wt% swelling. (9) and also water absorption capacities of up to 475 wt% for chitosan hydrogels with blue crab protein. Given this range, the values obtained for the BSG and SP protein hydrogels were relatively low, possibly due to the presence of GLA in the formulation. Although GLA can provide increased stability, the dense network formed within the hydrogel can restrict the entry of water molecules, thereby reducing water absorption capacities.

3.2. Physical integrity of hydrogels

Both before and after the swelling stage, the physical stability of the hydrogels was evaluated. Hydrogels with a 5% solid loading (70_3_5, 70_1_5, 50_3_5, and 50_1_5), as well as the center point samples (60_2_3) and the pure chitosan gels (CH-1, CH-2, and CH-3), demonstrated the most promising results in terms of mechanical integrity . During preparation, these gels formed a highly viscous, gel-like mixture upon the addition of both chitosan and crosslinker, indicating that the gelation point had been reached. This was attributed to the formation of a three-dimensional network structure within the hydrogel.

After lyophilization, these gels exhibited a styrofoam-like consistency (Fig. SX in the ESI). The gels were extremely lightweight and rigid, retaining shape under minimal pressure. However, the gels displayed limited elasticity, resulting in permanent cracks and indentations when subjected to higher pressure.

Once hydrated, these gels had a sponge-like consistency due to high porosity and visual texture (Fig. SX in the ESI), although the gels were slightly dense. High porosity is a desirable characteristic for adsorbents due to the increased surface area. Nevertheless, the gels were not soft and compressible, as such did not revert to original shape when heavily compressed. Despite this, the three-dimensional network structure of these hydrogels showed promising results in terms of physical stability, potentially enabling them to withstand adsorption capacity tests.

In contrast, hydrogels with a 1% solid loading (70_3_1, 70_1_1, 50_3_1, and 50_1_1) remained as slightly viscous liquids even after the addition of chitosan and crosslinker, indicating that the gelation point was not reached. The incomplete formation of the three-dimensional network could be due to the low percentage of solids in the gels. After lyophilization, these gels exhibited significantly low porosity, yet were lightweight, soft, and highly compressible. Once hydrated, these hydrogels barely maintained shape, displaying slimy and mucilaginous properties. Such characteristics are undesirable for conducting adsorption tests

due to the potential dissolution of the hydrogels when introduced into dye solutions.

Based on these findings regarding the physical stability and properties of the hydrogels, in conjunction with the water absorption capacity results, it was decided to eliminate the following hydrogels from the dye adsorption efficiency tests: 70_3_1, 70_1_1, 50_3_1, and 50_1_1.

3.3. Dye adsorption capacity and removal efficiency

Following the first elimination stage where water absorption capacity and physical stability of the hydrogels were considered, the dye adsorption capacity of the hydrogels was then evaluated with RB4 and MO solutions. These two anionic dyes were selected due to the structure (dichlorotriazine and azo dye) and utilization, serving as these relevant model molecules for dye adsorption (10,11). The results obtained during adsorption capacity and removal efficiency tests for the selected hydrogels, and with a 100 ppm RB4 solution, are presented in Table 1.

Table 1. Equilibrium adsorption capacity (q_e) and removal efficiency (R) for anionic dyes RB4 and MO with initial concentration of 100 ppm.

Dye	Sample	q_e (mg/g)	R (%)
RB4	70_3_5	41	88
	70_1_5	46	98
	50_3_5	42	91
	50_1_5	46	99
	60_2_3	40	87
	CH-1	39	85
	CH-2	39	84
	CH-3	40	85
MO	70_3_5	38	48
	70_1_5	55	70
	50_3_5	28	35
	50_1_5	44	56
	60_2_3	31	39
	CH-1	9	21
	CH-2	10	19
	CH-3	11	17

The addition of SPP resulted in superior adsorbance performance for both dyes, with samples 70_1_5 and 50_1_5 displaying nearly total removal efficiencies, of 98% and 99% for RB4, and 70% and 56% for MO, respectively. As mentioned prior, these two hydrogels presented the lowest concentration of crosslinker (1 wt%) during synthesis. Therefore, the availability of nucleophilic sites in both SPP and chitosan is higher to bind to the dyes. Qe values also correlated to the removal efficiencies with maximum values of 46 mg of RB4/g for and 55 mg of MO/g of hydrogel 70_1_5.

The SPP-chitosan hydrogels were more interactive towards RB4 compared to MO, this could be explained by the fact that reactive dyes present moieties that can potentially covalently bind to the adsorbent active sites. For instance, the dichlorotriazine moiety can be attacked by nucleophilic groups in the biocomposite hydrogels (12,13). MO, on the other hand, shares only the aromatic moieties and the sulfonate group for dye-adsorbent interactions.

3.3.3. Zeta potential and hydrogel selection

To further understand the difference in the hydrogels reactivity toward the dyes, the zeta potential (ζ) of both dyes was investigated. Additionally, the zeta potential of chitosan and SPP were also analysed and compared to understand the positive contribution provided by the squid pen protein to the adsorbents.

Zeta potential compares the difference between the surface potential of a particle to the potential of the liquid it is dispersed in. Therefore, this representation of surface change is useful when investigating how the dispersed particles interact with other surfaces (14).

The zeta potential values obtained were the following: for chitosan ζ= +14.85 mV, for squid pen protein ζ= +26.64 mV, for RB4 ζ= -16.32 mV, and for MO ζ= -39.79 mV.

Chitosan is a polycation, with the amino groups which can be easily protonated. Hence, it presents positive zeta potential values when dispersed that facilitate the adsorption of the dyes, which are negatively charged. In a study by Athavale et al. (2022) (15), the zeta potential values of chitosan nanoparticles produced were e between 12-25 mV, similar values to the values s obtained in this work.

The fact that SPP had a positive zeta potential in DI water means that the protein likely contained residual hydrochloric acid from the isoelectric precipitation. Protein isolates normally present positive zeta potential at low pH (2-4) and negative values at high pH (above 6) (16). Notably, the magnitude of SPP zeta potential was higher than the chitosan. The increase in surface charge resulted in stronger interactions between the hydrogel and dyes, and therefore higher adsorption capacity and dye removal efficiency results (15).

Both anionic dyes presented negative zeta potential values, which partly explains the efficacy of the biocomposites hydrogels and the dyes in terms of electrostatic interactions. Both dye molecules present sulphonic acid groups and therefore, their pKa is below 7. MO's pKa is 3.42, and RB4's first pKa is 0.8 (17)), which means that in DI water these molecules should be negatively charged. MO, however, presented relatively higher magnitude of zeta potential values, which suggest greater removal efficiency. Regarding such apparent discrepancy, it is also worth noting that while intermolecular and covalent bonds that can also play a role in the adsorption. RB4, as previously stated, can covalently bind to the adsorbent, which may explain the higher adsorption values.

Considering the adsorption capacity and removal efficiency results for both RB4 and MO solutions and the zeta potential values of the adsorbent components and dyes, both dyes were chosen as the probe dye for the adsorption isotherms. Additionally, hydrogels 70_1_5 and 50_1_5 were selected for adsorption isotherm analysis due to the superior performance of these formulations.

3.4. Adsorption isotherms

To characterize the adsorption behavior of samples 70_1_5 and 50_1_5 with both RB4 and MO solutions,

respective adsorption isotherms, based on Langmuir theory, were determined and analyzed. By plotting the experimentally obtained data of C_e and q_e according to the Langmuir model, Figures 1(a), (b), (c), and (d) were generated. Using the data from these plots and Equation (6), the Langmuir constants, K_L and α_L, were calculated. The linearity of each plot was evaluated based on the R^2 value of each trendline, which were 0.9762, 0.9685, 0.9875, and 0.9499 for Figures 1(a), (b), (c), and (d), respectively.

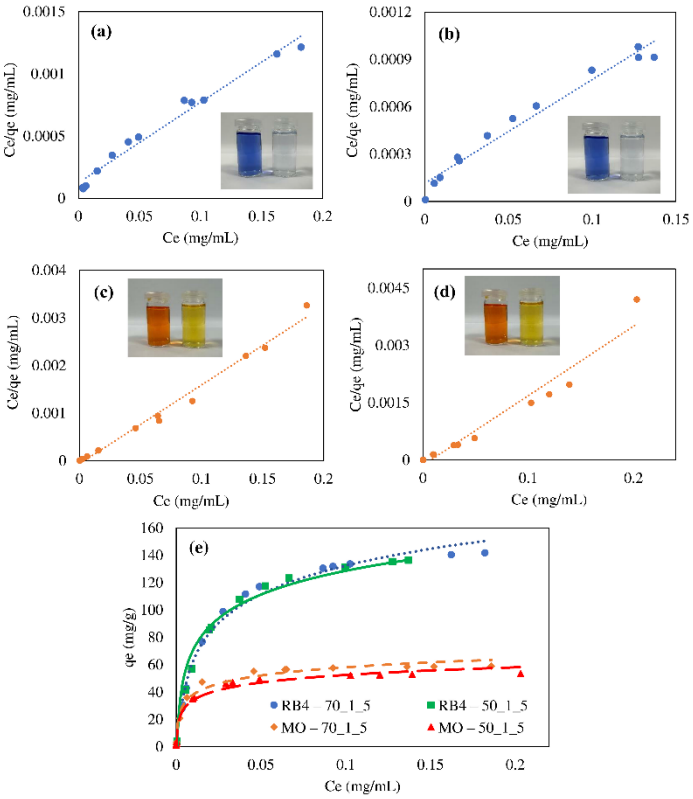

Figure 1. Equilibrium adsorption isotherms for 24 h treatment. (a) RB4 adsorption by hydrogel 70_1_5. (b) RB4 adsorption by hydrogel 50_1_5. (c) MO adsorption by hydrogel 70_1_5. (d) MO adsorption by 50_1_5 (e)Langmuir isotherms

Through the linearization of the experimental data, it was possible to plot the adsorption isotherms, following Langmuir theory, for both 70_1_5 and 50_1_5, with RB4 and MO solutions, as illustrated in Figure 1(e). The substantial adsorption capacity of both samples is evident in Figure 2, characterized by the sharp and steep initial increase, followed by a complete monolayer formation indicated by the plateau of each plot. In a work by Galan et al. (2021) (18) on the adsorption of RB4 with chitosan beads crosslinked with glutaraldehyde, a Freundlich isotherm was deemed as best linear fit for the adsorption process. This model posits that instead of a monolayer formation, there is a heterogeneous distribution of the active sites on the surfaces of the chitosan beads. Additionally, in a study by Zhai et al. (2017) on the adsorption of MO with chitosan microspheres (11), t the Langmuir model better described their adsorption process, which indicates similar behaviour to this work.

The calculated q_{max} values for the experiments RB4–70_1_5, RB4–50_1_5, MO–70_1_5, and MO–50_1_5, which were 153.85, 151.52, 60.24, and 54.94 mg/g, respectively. These q_{max} values for RB4 were superior to studies that also entailed producing bioadsorbents such as pure chitosan beads, q_{max} 1.56 mg/g, a chitosan and hydroxyapatite biocomposites, q_{max} 118.4, and 100% deacetylated chitosan, q_{max} 54.01. However, these were still inferior to studies that derivatised chitosan such as the works by(19–21). Regarding MO, similar trends were observed with underivatised chitosan hydrogels, q_{max} 10.53 and 12.46 mg/g in studies performed by (22,23), respectively. Whereas with modified chitosan biomaterials, such as the one produced by Chen et al. (2023) (24) with a cerium-based metal organic framework chitosan polyimine biocomposites, of q_{max} 900 mg/g.

3.5. Hydrogel characterisation

The samples' 70_1_5 and 50_1_5 chemical structure and surfaces were then characterised through Fourier transform infrared (FTIR) spectroscopy, optical microscopy and scanning electron microscopy imaging.

3.5.1. FT-IR spectroscopy

The FTIR spectra of dry hydrogels 70_1_5 and 50_1_5, illustrated in Figure 2a, show that both samples have the same absorption bands due to same composition. The most significant absorption bands were found at 3251, 2866, 2102, 1635, 1521, 1399, 1375, 1248, 1151, 1062, 1017 and 889 cm^{-1}, which were further characterised in Table 2 (ESI). Specifically, the amide I C=O stretching at 1635 cm^{-1} and the amide II N–H bending at 1511 cm^{-1} and the C–O–C and C–O stretching between 950-1200 cm^{-1} were also present, which are functional groups highly abundant in proteins, as also found in previous work. (26). Even though similar, it can be noticed that sample 70_1_5 presents higher intensity on the bands at 3251, 1635 and 1521 cm^{-1} which correspond to the higher content of chitosan. After RB4 dye adsorption, the spectra of dry 70_1_5 and 50_1_5 hydrogels were compared to the original spectra, as well as the RB4 powder spectra, it was hard to spot the absorption bands of the dye due to the poor absorbance of the material.

3.5.2. Optical microscopy and scanning electron microscopy (SEM)

SEM images of chitosan and hydrogel 50_1_5 are shown in Figure 2c and 2d. The surface of the chitosan hydrogel appeared rough and was composed of several microparticles of chitosan. On the other hand, the surface of the 50_1_5 hydrogel although still rough, seemed to be more homogeneously distributed, and the microparticles could not be distinguished. Images of samples 70_1_5 and 50_1_5 were taken before and after dye adsorption, with two different objective lenses to analyse the surfaces at various levels of detail. The presence of pores, ridges, and surface texture are crucial characteristics of an adsorbent since these provide a larger surface area. This therefore indicates that the hydrogel contains more binding sites for the dye molecules to adhere to, resulting in superior adsorption capacity. Previously, the roughness of bio polymer-based hydrogels was also observed with chitosan and gelatin hydrogels (27,28).

Optical microscopy images in Figure 2e and 2f show the presence of bubbles entrapped in the hydrogel's matrix, which can help to increase hydrogel their ential site adsorption.

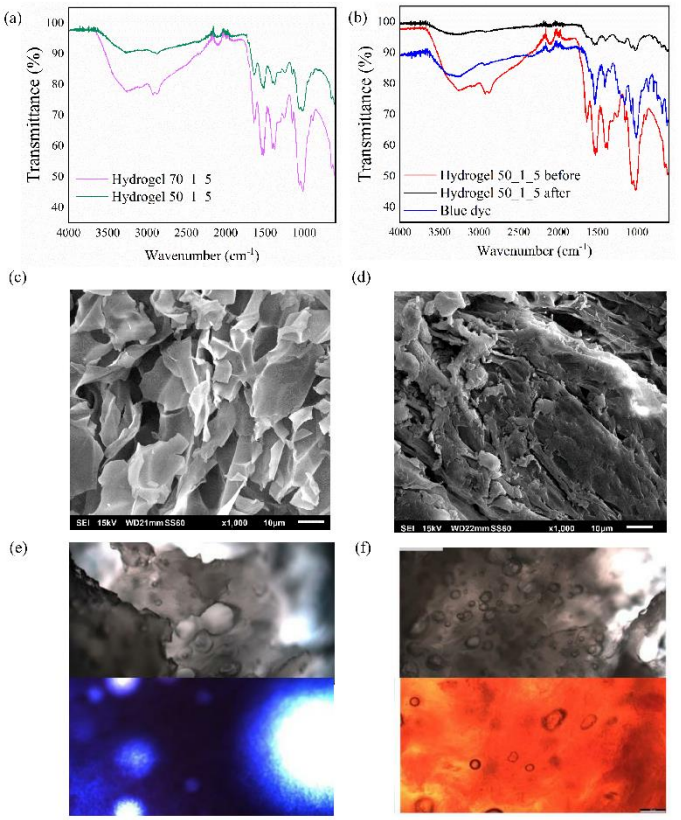

Figure 2. Characterisation of the hydrogels. (a) FT-IR spectra of the dry hydrogels. (b) RB4 adsorption by hydrogel 50_1_5 (before and after) (c) SEM of chitosan hydrogel with a x1000 magnification (d) SEM of hydrogel 50_1_5 with a x1000 magnification (e) Optical image of hydrogel 50_1_5 before and after RB4 adsorption (f) Optical image of hydrogel 50_1_5 before and after MO adsorption.

4. Conclusion

We produced biobased composites comprised of chitosan and squid pen protein. Chitosan was the structural matrix in which the squid protein pen protein was embedded . The functionality from the amino acid residues enhanced the extraction of two anionic dyes, RB4 and MO, with dye removal efficiencies of up to 99%. Higher crosslinker content negatively affected the adsorption performance due to the loss of potential binding nucleophilic sites from both the protein and chitosan. The combination of an alternative and cheap protein with chitosan into hydrogels paves the path for a more economically feasible wastewater treatment option.

ASSOCIATED CONTENT

Supporting Information. Materials and methods. Water absorption capacity of hydrogels. Hydrogels characterisation. "This material is available free of charge via the Internet at http://pubs.acs.org."

AUTHOR INFORMATION

Corresponding Author

* Pedro Nakasu

Author Contributions

The manuscript was written through contributions of all authors. All authors have given approval to the final version of the manuscript. Credit: **Pedro Nakasu‡:** conceptualization, supervision, draft writing; **Maite Martinez‡:** investigation, visualization, draft writing; **Talia Shmool:** supervision, draft reviewing and editing; **Susiana Melanie:** investigation; **Jason Hallet:** conceptualization, project administration, funding support, supervision, draft reviewing and editing. ‡These authors contributed equally.

Funding Sources

Supergen Bioenergy Impact Hub 2023 (EP/Y016300/1).

ACKNOWLEDGMENT

PYSN and JH are also grateful to the UKRI for support through the Supergen Bioenergy Impact Hub 2023 (EP/Y016300/1).

ABBREVIATIONS

GLA – Glutaraldehyde. MO – Methyl orange. SPP- Squid pen protein. RB4 -Reactive blue 4.

REFERENCES

1. Slama HB, Chenari Bouket A, Pourhassan Z, Alenezi FN, Silini A, Cherif-Silini H, et al. Diver-sity of Synthetic Dyes from Textile Industries, Discharge Impacts and Treatment Methods. Appl Sci. 2021 Jul 6;11(14):6255.

2. Vakili M, Rafatullah M, Salamatinia B, Abdullah AZ, Ibrahim MH, Tan KB, et al. Application of chitosan and its derivatives as adsorbents for dye removal from water and wastewater: a review. Carbohydr Polym. 2014 Nov 26;113:115–30.

3. Florowska A, Hilal A, Florowski T, Wroniak M. Addition of Selected Plant-Derived Proteins as Modifiers of Inulin Hydrogels Properties. Foods. 2020 Jun 29;9(7).

4. Strnad S, Zemljič LF. Cellulose-Chitosan Functional Biocomposites. Polymers (Basel). 2023 Jan 13;15(2).

5. Messerli MA, Raihan MJ, Kobylkevich BM, Benson AC, Bruening KS, Shribak M, et al. Con-struction and Composition of the Squid Pen from Doryteuthis pealeii. Biol Bull. 2019 Aug;237(1):1–15.

6. Riofrio A, Alcivar T, Baykara H. Environmental and Economic Viability of Chitosan Produc-tion in Guayas-Ecuador: A Robust Investment and Life Cycle Analysis. ACS Omega. 2021 Sep 14;6(36):23038–51.

7. Vo TS, Vo TTBC, Tran TT, Pham ND. Enhancement of water absorption capacity and com-pressibility of hydrogel sponges prepared from gelatin/chitosan matrix with different polyols. Progress in Natural Science: Materials International. 2022 Feb;32(1):54–62.

8. Jayanudin, Lestari RSD, Barleany DR, Pitaloka AB, Yulvianti M, Prasetyo D, et al. Chitosan-Graft-Poly(acrylic acid) Superabsorbent's Water Holding in Sandy Soils and Its Application in Agriculture. Polymers (Basel). 2022 Nov 28;14(23).

9. Hamdi M, Feki A, Bardaa S, Li S, Nagarajan S, Mellouli M, et al. A novel blue crab chi-tosan/protein composite hydrogel enriched with carotenoids endowed with distinguished wound healing capability: In vitro characterization and in vivo assessment. Mater Sci Eng C Mater Biol Appl. 2020 Aug;113:110978.

10. Subarna Karmaker, Nag AJ, Saha TK. Adsorption of Reactive Blue 4 Dye onto Chitosan 10B in Aqueous Solution: Kinetic Modeling and Isotherm Analysis. Russ J Phys Chem. 2020 Nov;94(11):2349–59.

11. Zhai L, Bai Z, Zhu Y, Wang B, Luo W. Fabrication of chitosan microspheres for efficient adsorption of methyl orange. Chin J Chem Eng. 2017 Sep;

12. Pei L, Liu J, Wang J. Study of dichlorotriazine reactive dye hydrolysis in siloxane reverse micro-emulsion. J Clean Prod. 2017 Nov;165:994–1004.

13. Soleimani-Gorgani A, Karami Z. The effect of biodegradable organic acids on the im-provement of cotton inkjet printing and antibacterial activity. Fibers Polym. 2016 Apr;17(4):512–20.

14. Dai M. The Effect of Zeta Potential of Activated Carbon on the Adsorption of Dyes from Aqueous Solution. J Colloid Interface Sci. 1994 Apr;164(1):223–8.

15. Athavale R, Sapre N, Rale V, Tongaonkar S, Manna G, Kulkarni A, et al. Tuning the surface charge properties of chitosan nanoparticles. Mater Lett. 2022 Feb;308:131114.

16. Freitas MLF, Albano KM, Telis VRN. Characterization of biopolymers and soy protein iso-late-high-methoxyl pectin complex. Polímeros. 2017 Mar;27(1):62–7.

17. Bagchi M, Ray L. Adsorption behavior of Reactive Blue 4, a tri-azine dye on dry cells of Rhizopus oryzae in a batch system. Chemical Speciation & Bioavailability. 2015 Jul 3;27(3):112–20.

18. Galan J, Trilleras J, Zapata PA, Arana VA, Grande-Tovar CD. Optimization of Chitosan Glu-taraldehyde-Cross-linked Beads for Reactive Blue 4 Anionic Dye Removal Using a Surface Response Methodology. Life (Basel). 2021 Jan 25;11(2).

19. Vakili M, Rafatullah M, Ibrahim MH, Abdullah AZ, Salamatinia B, Gholami Z. Chitosan hy-drogel beads impregnated with hexadecylamine for improved reactive blue 4 adsorption. Carbohydr Polym. 2016 Feb 10;137:139–46.

20. Vakili M, Rafatullah M, Salamatinia B, Ibrahim MH, Abdullah AZ. Elimination of reactive blue 4 from aqueous solutions using 3-aminopropyl triethoxysilane modified chitosan beads. Carbohydr Polym. 2015 Nov 5;132:89–96.

21. Vakili M, Rafatullah M, Ibrahim MH, Abdullah AZ, Gholami Z, Salamatinia B. Enhancing re-active blue 4 adsorption through chemical modification of chitosan with hexadecylamine and 3-aminopropyl triethoxysilane. Journal of Water Process Engineering. 2017 Feb;15:49–54.

22. Tamer TM, Sadik WA-A, Elady RA, Omer AM, Abd-El-latif MM, Mohy-Eldin MS. Novel amino-ethyl Chitosan hydrogel for methyl orange removal from waste water: Kinetics, isotherms, and thermodynamics studies. Desalination Water Treat. 2024 Jan;317:100122.

23. Alyasi H, Mackey H, McKay G. Adsorption of Methyl Orange from Water Using Chitosan Bead-like Materials. Molecules. 2023 Sep 11;28(18).

24. Chen Z, Zhang Z-B, Zeng J, Zhang Z-J, Ma S, Tang C-M, et al. Preparation of polyethylene-imine-modified chitosan/Ce-UIO-66 composite hydrogel for the adsorption of methyl or-ange. Carbohydr Polym. 2023 Jan 1;299:120079.

25. Acosta-Ferreira S, Castillo OS, Madera-Santana JT, Mendoza-García DA, Núñez-Colín CA, Grijalva-Verdugo C, et al. Production and physicochemical characterization of chitosan for the harvesting of wild microalgae consortia. Biotechnol Rep (Amst). 2020 Dec;28:e00554.

26. Cuong HN, Minh NC, Van Hoa N, Trung TS. Preparation and characterization of high puri-ty β-chitin from squid pens (Loligo chenisis). Int J Biol Macromol. 2016 Dec;93(Pt A):442–7.

27. Samal SK, Dash M, Chiellini F, Wang X, Chiellini E, Declercq HA, et al. Silk/chitosan biohy-brid hydrogels and scaffolds via green technology. RSC Adv. 2014;4(96):53547–56.

28. Shengjie Li, Zhuo Xiong, Xiaohong Wang, Yongnian Yan, Haixia Liu, Renji Zhang. Direct Fabrication of a Hybrid Cell/Hydrogel Construct by a Double-nozzle Assembling Technol-ogy. J Bioact Compat Polym. 2009 May 1;24(3):249–65.

Authors are required to submit a graphic entry for the Table of Contents (TOC) that, in conjunction with the manuscript title, should give the reader a representative idea of one of the following: A key structure, reaction, equation, concept, or theorem, etc., that is discussed in the manuscript. Consult the journal's Instructions for Authors for TOC graphic specifications.

Insert Table of Contents artwork here